Fractional Calculus & Applied Analysis
An International Journal for Theory and Applications
VOLUME 22, NUMBER 5 (2019)
(Print) ISSN 1311-0454
(Electronic) ISSN 1314-2224

RESEARCH PAPER

NUMERICAL SOLUTION OF FRACTIONAL-ORDER ORDINARY DIFFERENTIAL EQUATIONS USING THE REFORMULATED INFINITE STATE REPRESENTATION

Matthias Hinze [1], **André Schmidt** [1], **Remco I. Leine** [1]

Abstract

In this paper, we propose a novel approach for the numerical solution of fractional-order ordinary differential equations. The method is based on the infinite state representation of the Caputo fractional differential operator, in which the entire history of the state of the system is considered for correct initialization. The infinite state representation contains an improper integral with respect to frequency, expressing the history dependence of the fractional derivative. The integral generally has a weakly singular kernel, which may lead to problems in numerical computations. A reformulation of the integral generates a kernel that decays to zero at both ends of the integration interval leading to better convergence properties of the related numerical scheme. We compare our method to other schemes by considering several benchmark problems.

MSC 2010: 34A08, 34K28, 65L03

Key Words and Phrases: fractional derivatives; fractional ordinary differential equations; infinite state representation; diffusive representation; benchmark problems

pp. 1321–1350 , DOI: 10.1515/fca-2019-0070 DE GRUYTER

1. Introduction

This paper presents a novel numerical method for the solution of fractional-order ordinary differential equations (FODEs) by exploiting a reformulation of the infinite state representation, which has originally been developed in the context of Lyapunov stability theory.

FODEs are considered within the theory of fractional calculus, which is a mathematical field dealing with derivatives and integrals of arbitrary (non-integer) order [6, 27] with a variety of applications. Particularly in mechanics, fractional damping may arise through the modeling of mechanical systems with viscoelastic components. Complex rheological models for viscoelastic materials are often described through an array of classical Kelvin or Maxwell elements (i.e. elements containing derivatives of integer order), inevitably resulting in a model with a large number of parameters. It has been shown that the viscoelastic behavior of complex materials in many applications is well represented by fractional-order elements, so called 'springpots', with only a few parameters [2, 30]. Actually, a springpot may be interpreted as an infinite series of Kelvin or Maxwell elements [15, 16, 26, 28]. This analogy can be expressed by using the infinite state representation (also called diffusive representation) of fractional derivatives and integrals introduced in [23, 24]. Furthermore, this idea leads to a potential energy representation for a springpot [16, 34] which in turn can be used to prove stability of equilibria for fractionally damped mechanical systems. In this context, a reformulation of the infinite state representation of fractional derivatives has been developed, which extracts both the energy preserving and dissipating components of a springpot [17]. This naturally leads to a Lyapunov functional for the rigorous proof of Lyapunov stability of equilibria for a class of mechanical systems with fractional damping.

The infinite state representation is widely spread in numerical methods dealing with fractional derivatives and integrals [32, 35, 39], as this approach leads to systems of integer-order instead of fractional differential equations. In contrast to direct approaches to solve fractional differential equations [9, 11, 22], these methods do not require to process the entire solution history in every time step which leads to a substantial reduction of computational costs and memory requirements. The accuracy of the approximation based on the infinite state representation is impaired by the presence of a weakly singular kernel. Furthermore, the accuracy depends on the chosen quadrature [1, 18, 20, 39] and the order of differentiation [1, 18, 20] whereas the prediction of the asymptotic behavior may be incorrect [29].

In this contribution, we propose to exploit the reformulation of the fractional derivative introduced in [17], which leads to a non-singular integration kernel that asymptotically decays to zero. Therefore, the related scheme, which uses a Gauss-Legendre quadrature, causes small truncation and quadrature errors of the infinite state integral. The performance of the proposed scheme is studied in comparison to existing numerical methods for several benchmark problems related to the problems in [37, 38].

In Sect. 2 we set notation for FODEs and the infinite state representation of Caputo fractional derivatives. Sect. 3 describes a classical scheme to handle (special types of) FODEs and several methods based on the infinite state representation. The reformulation of the infinite state representation is presented in Sect. 4. Based on the reformulation, we derive a numerical scheme and give a brief error analysis. In Sect. 5 we consider a set of benchmark problems and compare our scheme to the existing methods from Sect. 3. Finally, in Sect. 6 we draw conclusions and state some generalizations of the proposed method.

2. Fractional derivatives and fractional-order ordinary differential equations

We consider the Caputo derivative of order $\alpha \in (0,1)$ of a continuously differentiable real-valued function $q(t)$ as

$$ {}^{C}D^{\alpha}_{t_0+} q(t) = \frac{1}{\Gamma(1-\alpha)} \int_{t_0}^{t} (t-\tau)^{-\alpha} \dot{q}(\tau) \mathrm{d}\tau \tag{2.1} $$

with the Gamma function

$$ \Gamma(\alpha) = \int_0^{\infty} u^{\alpha-1} \mathrm{e}^{-u} \mathrm{d}u. \tag{2.2} $$

As initialization time instant $t_0 \in [-\infty, 0]$ we consider the beginning of the non-zero history of $q(t)$, i.e. $q(t) = \dot{q}(t) = 0$ for $t \leq t_0$ and we think of $t = 0$ as initial time instant. Accordingly, we consider an initialized fractional derivative of q similar as in [21]. Note that the initialization time instant t_0 is a property of (the history of) the function q and not of the differential operator. The definition (2.1) is related to the fractional Riemann-Liouville integral

$$ I^{\alpha}_{t_0+} q(t) = \frac{1}{\Gamma(\alpha)} \int_{t_0}^{t} (t-\tau)^{\alpha-1} q(\tau) \mathrm{d}\tau \tag{2.3} $$

by

$$ {}^{C}D^{\alpha}_{t_0+} q(t) = I^{1-\alpha}_{t_0+} \dot{q}(t). \tag{2.4} $$

An equation of the form

$$ \begin{aligned} &A q^{(n)}(t) + B\, {}^{C}D^{\alpha_{n-1}}_{t_0+} q^{(n-1)}(t) \\ &\qquad = F\left(t, q(t), {}^{C}D^{\alpha_0}_{t_0+} q(t), \dot{q}(t), \ldots, {}^{C}D^{\alpha_{n-2}}_{t_0+} q^{(n-2)}(t), q^{(n-1)}(t)\right) \end{aligned} \tag{2.5} $$

is denoted as an (explicit) fractional-order ordinary differential equation (FODE) of order $n \in \mathbb{N}$ (or $n-1+\alpha_{n-1}$ for $A = 0$), with $A, B \in \mathbb{R}$, $A \vee B \neq 0$ and fractional orders $\alpha_0, \ldots, \alpha_{n-1} \in (0,1)$. More generally, q may have values in $\mathbb{R}^m$. In this case $q = (q_1, \ldots, q_m)^{\mathrm{T}} \in \mathbb{R}^m$ is a vector, $A, B \in \mathbb{R}^{m \times m}$ are matrices and $\alpha_i = (\alpha_{i,1}, \ldots, \alpha_{i,m})^{\mathrm{T}} \in (0,1)^m$, $i = 0, \ldots, n-1$ are multi-orders such that

$$ {}^{C}D^{\alpha_i}_{t_0+} q^{(i)}(t) = \left({}^{C}D^{\alpha_{i,1}}_{t_0+} q_1^{(i)}(t), \ldots, {}^{C}D^{\alpha_{i,m}}_{t_0+} q_m^{(i)}(t) \right)^{\mathrm{T}}. \tag{2.6} $$

In contrast to the classical approach, we will equip an FODE with an initial function $q(t) = q_0(t)$ for $t \in (t_0, 0)$ instead of initial values at one time instant. Thus, we relate an FODE to an equivalent functional or Volterra integro-differential equation with unbounded delay in the sense of [3, 14, 19].

In the following, we will use another representation of the operator (2.1), which is called infinite state or diffusive representation [23, 24, 35] and can be written as the infinite state integral

$$ {}^{C}D^{\alpha}_{t_0+} q(t) = \int_0^\infty \mu_{1-\alpha}(\omega) y(\omega, t) \mathrm{d}\omega, \tag{2.7} $$

where the function μ_α is defined as

$$ \mu_\alpha(\eta) := \frac{\sin(\alpha\pi)}{\pi} \eta^{-\alpha} \tag{2.8} $$

and the infinite states $y(\eta, t)$, $\eta \in (0, \infty)$ solve the initial value problem

$$ \dot{y}(\eta, t) = -\eta y(\eta, t) + \dot{q}(t), \quad y(\eta, 0) = \int_{t_0}^0 \mathrm{e}^{\eta\tau} \dot{q}(\tau) \mathrm{d}\tau. \tag{2.9} $$

To see (2.7), we use (2.2) and obtain

$$ \frac{t^{-\alpha}}{\Gamma(1-\alpha)} = \frac{1}{\Gamma(\alpha)\Gamma(1-\alpha)} \int_0^\infty t^{-\alpha} u^{\alpha-1} \mathrm{e}^{-u} \mathrm{d}u = \int_0^\infty \mu_{1-\alpha}(\omega) \mathrm{e}^{-\omega t} \mathrm{d}\omega, \tag{2.10} $$

where we substitute $u = \omega t$ and use the property

$$ \Gamma(\alpha)\Gamma(1-\alpha) = \frac{\pi}{\sin(\alpha\pi)}. \tag{2.11} $$

We obtain Eq. (2.7) by inserting (2.10) in (2.1), using Fubini's theorem and the solution of (2.9). Using the representation (2.7) together with (2.9) translates the fractional derivatives in Eq. (2.5) to integer-order. Furthermore, the initial function q_0 is transferred to initial conditions of the infinite states

$$ y(\eta, 0) = \int_{t_0}^0 \mathrm{e}^{\eta\tau} \dot{q}_0(\tau) \mathrm{d}\tau. \tag{2.12} $$

In this sense, an FODE may be understood as an infinite-dimensional ODE. Hence, an FODE may also be approximated by an ODE of high (but finite)

dimension, being the key idea behind the infinite state based schemes of Sect. 3.2 and the novel scheme in Sect. 4.

3. Two kinds of numerical schemes for FODEs

In this section, we will give a brief introduction to a classical and some infinite state based numerical schemes to solve (special types of) FODEs as we want to compare these methods to the novel scheme proposed in Sect. 4.

3.1. **Predictor-Corrector-Scheme.** A classical method to solve fractional initial-value problems of the form

$$\begin{cases} {}^{C}D^{\alpha}_{t_0+}q(t) = f(t, q(t)), & m-1 < \alpha \le m, \\ q^{(k)}(0) = q_0^{(k)}, & k = 0, 1, \dots, m-1, \end{cases} \tag{3.1}$$

for $t \in [0, T]$ is the predictor-corrector-scheme (PC) proposed in [9] and extensively analyzed in [10]. Notice that in this scheme a fractional differential equation is considered together with initial values instead of an initial function. The method is applied to the integral form of (3.1) being

$$q(t) = \sum_{k=0}^{\lceil\alpha\rceil-1} q_0^{(k)} \frac{t^k}{k!} + \frac{1}{\Gamma(\alpha)} \int_0^t (t-\tau)^{\alpha-1} f(\tau, q(\tau)) d\tau. \tag{3.2}$$

The integral in (3.2) is approximated by a composite trapezoidal rule with fixed time-step $h = t_j - t_{j-1}$, $j = 1, \dots, N = \lfloor \frac{T}{h} \rfloor$ which leads to

$$\tilde{q}(t_{n+1}) = \sum_{k=0}^{\lceil\alpha\rceil-1} q_0^{(k)} \frac{t_{n+1}^k}{k!} + \frac{h^\alpha}{\Gamma(\alpha+2)} \sum_{j=0}^{n+1} a_{j,n+1} f(t_j, \tilde{q}(t_j)) \tag{3.3}$$

with coefficients

$$a_{j,n+1} = \begin{cases} n^{\alpha+1} - (n-\alpha)(n+1)^\alpha & j = 0, \\ (n-j+2)^{\alpha+1} + (n-j)^{\alpha+1} - 2(n-j+1)^{\alpha+1} & 1 \le j \le n, \\ 1 & j = n+1. \end{cases} \tag{3.4}$$

To avoid solving the nonlinear equation (3.3) for $\tilde{q}(t_{n+1})$, the solution is estimated in a predictor step with the help of the (explicit) rectangular rule as

$$\tilde{q}^p(t_{n+1}) = \sum_{k=0}^{\lceil\alpha\rceil-1} q_0^{(k)} \frac{t_{n+1}^k}{k!} + \frac{1}{\Gamma(\alpha)} \sum_{j=0}^{n} b_{j,n+1} f(t_j, \tilde{q}(t_j)) \tag{3.5}$$

with coefficients

$$b_{j,n+1} = \frac{h^\alpha}{\alpha}((n+1-j)^\alpha - (n-j)^\alpha)$$

and corrected by (3.3) as

$$\begin{aligned}\tilde{q}(t_{n+1}) = &\sum_{k=0}^{\lceil\alpha\rceil-1} q_0^{(k)} \frac{t_{n+1}^k}{k!} + \frac{h^\alpha}{\Gamma(\alpha+2)} f(t_{n+1}, \tilde{q}^p(t_{n+1})) \\ &+ \frac{h^\alpha}{\Gamma(\alpha+2)} \sum_{j=0}^{n} a_{j,n+1} f(t_j, \tilde{q}(t_j)).\end{aligned} \tag{3.6}$$

The scheme leads to an error estimation

$$\max_{j=0,1,\ldots,N} |q(t_j) - \tilde{q}(t_j)| = \mathcal{O}(h^p), \quad p = \min(2, 1+\alpha), \quad (h \to 0). \tag{3.7}$$

The method may be directly applied to FODEs with rational derivation orders $\alpha_0, \ldots, \alpha_{n-1}$ in (2.5). To this end, (2.5) is transferred to a vectorial version of (3.1), where α is the greatest common divisor of $\alpha_0, \ldots, \alpha_{n-1}$. In the general case, the irrational derivation orders in the set $\{\alpha_0, \ldots, \alpha_{n-1}\}$ have to be approximated by rational ones. The details may be found in [8] and [9, Sec. 4]. The algorithm may be improved, e.g. using several corrector iterations or applying Richardson extrapolation [9, Sec. 3]. In Sect. 5, we test this algorithm using the implementation `fde12.m`, [12].

3.2. **Infinite state based methods.** Methods based on the infinite state representation (2.7) of the fractional derivative usually start with a discretization of the infinite states and a related quadrature of the improper integral in (2.7), which leads to a representation

$$\begin{aligned}\widetilde{{}^C D_{t_0+}^\alpha q(t)} &= \sum_{n=0}^{N} y_n(t) w_n, \\ \dot{y}_n(t) &= \dot{q}(t) - \eta_n y_n(t), \quad n = 0, \ldots, N,\end{aligned} \tag{3.8}$$

with $y_n(t) = y(\eta_n, t)$. Alternatively, the infinite state representation of the fractional Riemann-Liouville integral (2.3) of the form

$$\begin{aligned}I_{t_0+}^\alpha q(t) &= \int_0^\infty \mu_\alpha(\omega) Z(\omega, t) \mathrm{d}\omega, \\ \dot{Z}(\eta, t) &= q(t) - \eta Z(\eta, t)\end{aligned} \tag{3.9}$$

may be discretized as

$$\begin{aligned}\widetilde{I_{t_0+}^\alpha q(t)} &= \sum_{n=0}^{N} Z_n(t) w_n, \\ \dot{Z}_n(t) &= q(t) - \eta_n Z_n(t), \quad n = 0, \ldots, N\end{aligned} \tag{3.10}$$

with $Z_n(t) = Z(\eta_n, t)$. Thereby, the discrete values η_n and w_n, $n = 0, \ldots, N$ are the nodes and weights of the chosen quadrature, respectively, where the kernel μ is incorporated in the weights w_n. The approximations (3.8) and

(3.10) bring forth two difficulties: The upper bound of the integral is infinite and the kernel μ is weakly singular at zero. Both facts have to be considered when choosing the quadrature. Furthermore, the substitution of (3.8) into an FODE (2.5) leads to a stiff ODE (while the substitution of (3.10) in a fractional integral equation leads to a stiff DAE), asking for a dedicated stiff solver. Originally, an infinite state scheme of the form (3.10) is used in [33, 35] together with an adapted version of Oustaloup's filter [25] to perform the quadrature. The frequencies η_n are in this case chosen to be geometrically distributed, i.e. equidistant on a logarithmic scale. In the much-debated articles [4, 39], transformed representations similar to (3.8) are introduced. The quadrature used in [39] is of Gauss-Laguerre type, which is adapted to the improper integral in (2.7). However, the weak singularity is not considered in this approach and the asymptotic decay of the integrand for $\omega \to \infty$ is rather slow, which leads to slow convergence of the scheme [7]. A significant improvement may be obtained using a Gauss-Jacobi quadrature for a transformed infinite state integral [7], which considers the weak singularity at zero. Alternatively, the use of a Galerkin method was proposed in [7, 32]. Recently, several schemes using composite quadrature rules have been introduced, e.g. in [20] (composite Gauss-Legendre) and [1, 18] (composite Gauss-Jacobi). These schemes use the advantage, that particular subintervals, usually distributed over many decades, may be chosen in advance to perform the quadrature on each interval (whereas in a single Gaussian quadrature the nodes are only determined by the zeroes of certain orthogonal polynomials).

In the following, we will describe a composite Gauss-Jacobi quadrature for (3.10) similar to the quadrature of the scheme in [1], as we will compare its results to the method proposed in Sect. 4. When using this scheme in Sect. 5, we will refer to it as the infinite state scheme (ISS). A general Gauss-Jacobi quadrature is an approximation of an integral over the interval $[-1, 1]$ of a continuous function f weighted by an algebraic function with (possibly) weak singularities at the boundaries of the integration interval. It has the form

$$\int_{-1}^{1} (1+x)^{\beta}(1-x)^{\gamma} f(x)\mathrm{d}x \approx \sum_{n=0}^{N} f\left(s_n^{(\beta,\gamma)}\right) w_n^{(\beta,\gamma)} \tag{3.11}$$

with $\beta, \gamma > -1$, nodes $s_n^{(\beta,\gamma)}$ and weights $w_n^{(\beta,\gamma)}$ such that polynomials of degree $2N-1$ are integrated exactly. The details on determining the nodes and weights may be found e.g. in [5, Ch. 2.7]. In the present case, we will use a composite version of this idea, i.e. we choose $\eta_0 = 0$, $\eta_1, \ldots, \eta_K$ in $(0, \infty)$ and perform a Gauss-Jacobi quadrature in each interval

$(\eta_0, \eta_1), \ldots, (\eta_{K-1}, \eta_K)$ with nodes $\eta_{k,j} \in (\eta_k, \eta_{k+1})$ and weights $w_j^{(\beta_k,\gamma_k)}$, $j = 1, \ldots, J$, $k = 0, \ldots, K-1$. We use a substitution

$$\begin{aligned}\int_a^b (x-a)^\beta (b-x)^\gamma f(x) \mathrm{d}x &= \left(\frac{b-a}{2}\right)^{1+\beta+\gamma} \int_{-1}^{1} (1+s)^\beta (1-s)^\gamma f\left(\frac{b-a}{2}s + \frac{a+b}{2}\right) \mathrm{d}s \\ &\approx \left(\frac{b-a}{2}\right)^{1+\beta+\gamma} \sum_{n=0}^{N} f\left(\frac{b-a}{2} s_n^{(\beta,\gamma)} + \frac{a+b}{2}\right) w_n^{(\beta,\gamma)}\end{aligned} \tag{3.12}$$

to adapt to the integration boundaries $a < b$. Applying this procedure to (3.9) leads to

$$\begin{aligned}\int_0^{\eta_1} \mu_\alpha(\omega) Z(\omega,t) \mathrm{d}\omega &= \frac{\sin(\alpha\pi)}{\pi} \int_0^{\eta_1} \omega^{-\alpha} Z(\omega,t) \mathrm{d}\omega \\ &= \frac{\sin(\alpha\pi)}{\pi} \left(\frac{\eta_1}{2}\right)^{1-\alpha} \int_{-1}^{1} (1+s)^{-\alpha} Z\left(\frac{\eta_1}{2}(1+s), t\right) \mathrm{d}s \\ &\approx \frac{\sin(\alpha\pi)}{\pi} \left(\frac{\eta_1}{2}\right)^{1-\alpha} \sum_{j=1}^{J} Z\Bigg(\underbrace{\frac{\eta_1}{2}\left(1+s_j^{(-\alpha,0)}\right)}_{=:\eta_{0,j}}, t\Bigg) w_j^{(-\alpha,0)}\end{aligned} \tag{3.13}$$

and, using the abbreviation $\eta_k(s) = \frac{\eta_{k+1}-\eta_k}{2}s + \frac{\eta_k+\eta_{k+1}}{2}$

$$\begin{aligned}\int_{\eta_k}^{\eta_{k+1}} \mu_\alpha(\omega) Z(\omega,t) \mathrm{d}\omega &= \frac{\eta_{k+1}-\eta_k}{2} \int_{-1}^{1} \mu_\alpha(\eta_k(s)) Z(\eta_k(s), t) \mathrm{d}s \\ &\approx \frac{\eta_{k+1}-\eta_k}{2} \sum_{j=1}^{J} \mu_\alpha\left(\eta_k\left(s_j^{(0,0)}\right)\right) Z\left(\eta_k\left(s_j^{(0,0)}\right), t\right) w_j^{(0,0)} \\ &= \frac{\eta_{k+1}-\eta_k}{2} \sum_{j=1}^{J} \mu_\alpha(\eta_{k,j}) Z(\eta_{k,j}, t) w_j^{(0,0)}\end{aligned} \tag{3.14}$$

for $k = 1, \ldots, K-1$, where $\eta_{k,j} = \eta_k\left(s_j^{(0,0)}\right)$. Hence, we only have to compute one set of nodes and weights

$$\left(s_j^{(-\alpha,0)}, w_j^{(-\alpha,0)}\right)_{j=1,\ldots,J} \tag{3.15}$$

for the quadrature in (3.13) and another set

$$\left(s_j^{(0,0)}, w_j^{(0,0)}\right)_{j=1,\ldots,J} \tag{3.16}$$

for the case (3.14), which is independent of $k \in \{1, \dots, K-1\}$. Actually, the weak singularity only has to be considered in (3.13), while more specifically (3.14) represents a Gauss-Legendre quadrature. In summary, we obtain the approximation

$$\begin{aligned}\int_0^\infty \mu_\alpha(\omega) Z(\omega,t)\mathrm{d}\omega \approx \frac{\sin(\alpha\pi)}{\pi}\left(\frac{\eta_1}{2}\right)^{1-\alpha}\sum_{j=1}^{J} Z(\eta_{0,j},t)w_j^{(-\alpha,0)} \\ + \sum_{k=1}^{K-1}\frac{\eta_{k+1}-\eta_k}{2}\sum_{j=1}^{J}\mu_\alpha(\eta_{k,j})Z(\eta_{k,j},t)w_j^{(0,0)}\end{aligned} \tag{3.17}$$

of (3.9), which may be used in (3.10), where $N = K \cdot J$. To use this approximation for solving a fractional integral equation, we still have to choose an appropriate DAE solver. As the coefficients η_n of Y_n in the ODEs of (3.10) become huge numbers for large n, the resulting DAEs will usually be stiff, such that explicit time stepping methods fail [7, Sec. 3.2]. Therefore, in our numerical examples, we will use MATLAB's stiff solver `ode15s.m`, which uses an implicit method (BDF).

4. Reformulated infinite state scheme

4.1. Reformulation of the infinite state representation.

As discussed in Sect. 3.2, the asymptotic behavior of the integrand may lead to problems in the infinite state based methods that we want to overcome using a reformulation of (2.7). Therefore, we propose to consider a second kind of infinite states $Y(\eta,t)$, $\eta \in (0,\infty)$ that fulfill

$$\dot{Y}(\eta,t) = -\eta Y(\eta,t) + q(t), \quad Y(\eta,0) = \int_{t_0}^{0} \mathrm{e}^{\eta\tau} q(\tau)\mathrm{d}\tau \tag{4.1}$$

and $\dot{Y} = y$. In the following, we will introduce an expansion of the integration kernel in (2.7) by the term $\omega^2 + r^2$ for a real number $r > 0$. The following properties will prove to be useful in the proposed reformulation.

Proposition 4.1.

$$\int_0^\infty \frac{\mu_\alpha(\omega)}{\omega + s}\mathrm{d}\omega = s^{-\alpha}, \quad s \in \mathbb{C}\backslash\mathbb{R}^-,\ \alpha \in (0,1). \tag{4.2}$$

P r o o f. Making use of the Laplace transform of $\mathrm{e}^{-\omega t}$

$$\begin{aligned}\mathcal{L}\{\mathrm{e}^{-\omega t}\}(s) &= \int_0^\infty \mathrm{e}^{-\omega t}\mathrm{e}^{-st}\mathrm{d}t = \int_0^\infty \mathrm{e}^{-(\omega+s)t}\mathrm{d}t \\ &= \left[-\frac{1}{\omega+s}\mathrm{e}^{-(\omega+s)t}\right]_0^\infty = \frac{1}{\omega+s},\end{aligned}$$

we obtain Eq. (4.2) using Fubini's theorem and (2.11) as

$$\begin{aligned}\int_0^\infty \frac{\mu_\alpha(\omega)}{\omega+s}\mathrm{d}\omega &= \frac{\sin(\alpha\pi)}{\pi}\int_0^\infty \omega^{-\alpha}\int_0^\infty \mathrm{e}^{-(\omega+s)t}\mathrm{d}t\mathrm{d}\omega \\ &= \frac{\sin(\alpha\pi)}{\pi}\int_0^\infty \mathrm{e}^{-st}\int_0^\infty \omega^{-\alpha}\mathrm{e}^{-\omega t}\mathrm{d}\omega\mathrm{d}t \\ &= \frac{\sin(\alpha\pi)}{\pi}\int_0^\infty \mathrm{e}^{-st}\Gamma(1-\alpha)t^{\alpha-1}\mathrm{d}t \\ &= \frac{\sin(\alpha\pi)}{\pi}\Gamma(1-\alpha)\Gamma(\alpha)s^{-\alpha} = s^{-\alpha}.\end{aligned}$$

□

Remark 4.1. The result of Prop. 4.1 is also used in [35] (without proof). A similar proof as the one given here may be found in [36].

Proposition 4.2. *For $\alpha \in (0,1)$ and $r > 0$, the identities*

$$\int_0^\infty \frac{\mu_{1-\alpha}(\omega)}{\omega^2+r^2}\mathrm{d}\omega = \cos\left(\frac{\alpha\pi}{2}\right) r^{\alpha-2}, \tag{4.3}$$

$$\int_0^\infty \frac{\mu_{1-\alpha}(\omega)\omega}{\omega^2+r^2}\mathrm{d}\omega = \sin\left(\frac{\alpha\pi}{2}\right) r^{\alpha-1} \tag{4.4}$$

hold.

P r o o f. Substitute $\eta = \omega^2$ and $\mathrm{d}\eta = 2\omega\,\mathrm{d}\omega$ in the integral and obtain

$$\begin{aligned}\int_0^\infty \frac{\mu_{1-\alpha}(\omega)}{\omega^2+r^2}\mathrm{d}\omega &= \frac{\sin(\alpha\pi)}{\pi}\int_0^\infty \frac{\omega^{\alpha-1}}{\omega^2+r^2}\mathrm{d}\omega = \frac{\sin(\alpha\pi)}{2\pi}\int_0^\infty \frac{\eta^{\frac{\alpha}{2}-1}}{\eta+r^2}\mathrm{d}\eta \\ &= \frac{\sin(\alpha\pi)}{2\sin\left(\frac{\alpha\pi}{2}\right)}\int_0^\infty \frac{\mu_{1-\frac{\alpha}{2}}(\eta)}{\eta+r^2}\mathrm{d}\eta.\end{aligned}$$

Using the sine-double-angle formula and (4.2), we directly obtain (4.3). The proof of (4.4) is analogous. □

Expansion of (2.7) by the term $\omega^2 + r^2$ for a fixed $r > 0$ leads together with (2.9), (4.1), (4.3) and (4.4) to

$$
\begin{aligned}
{}^{C}D^{\alpha}_{t_0+}q(t) &= \int_0^\infty \frac{\mu_{1-\alpha}(\omega)\omega}{\omega^2+r^2}\omega y(\omega,t)\mathrm{d}\omega + r^2\int_0^\infty \frac{\mu_{1-\alpha}(\omega)}{\omega^2+r^2}y(\omega,t)\mathrm{d}\omega \\
&= \int_0^\infty \frac{\mu_{1-\alpha}(\omega)\omega}{\omega^2+r^2}\mathrm{d}\omega\,\dot{q}(t) - \int_0^\infty \frac{\mu_{1-\alpha}(\omega)\omega}{\omega^2+r^2}\dot{y}(\omega,t)\mathrm{d}\omega \\
&\quad + r^2\int_0^\infty \frac{\mu_{1-\alpha}(\omega)}{\omega^2+r^2}\mathrm{d}\omega\,q(t) - r^2\int_0^\infty \frac{\mu_{1-\alpha}(\omega)\omega}{\omega^2+r^2}Y(\omega,t)\mathrm{d}\omega \qquad (4.5)\\
&= \sin\left(\frac{\alpha\pi}{2}\right) r^{\alpha-1}\dot{q}(t) - \int_0^\infty \frac{\mu_{1-\alpha}(\omega)\omega}{\omega^2+r^2}\dot{y}(\omega,t)\mathrm{d}\omega \\
&\quad + \cos\left(\frac{\alpha\pi}{2}\right) r^{\alpha}q(t) - r^2\int_0^\infty \frac{\mu_{1-\alpha}(\omega)\omega}{\omega^2+r^2}Y(\omega,t)\mathrm{d}\omega.
\end{aligned}
$$

The advantage of this reformulation of the fractional derivative is the new kernel with parameter $r > 0$

$$
\mathrm{K}(\alpha,\eta) = \frac{\mu_{1-\alpha}(\eta)\eta}{\eta^2+r^2} = \frac{\sin(\alpha\pi)}{\pi}\frac{\eta^\alpha}{\eta^2+r^2}, \qquad (4.6)
$$

that is integrable on $\mathbb{R}_0^+$ and fulfills

$$
\lim_{\eta\to 0}\mathrm{K}(\alpha,\eta) = \lim_{\eta\to\infty}\mathrm{K}(\alpha,\eta) = 0, \quad \alpha\in(0,1). \qquad (4.7)
$$

Furthermore, (4.5) contains only first-order derivatives of q and the infinite states y and Y, being key to our numerical scheme which is based on the solution of high-dimensional ODEs. Regarding (2.5), which contains several fractional orders α_i, we generalize (4.5) to

$$
\begin{aligned}
{}^{C}D^{\alpha_i}_{t_0+}q^{(i)}(t) &= \sin\left(\frac{\alpha_i\pi}{2}\right) r^{\alpha_i-1}q^{(i+1)}(t) - \int_0^\infty \mathrm{K}(\alpha_i,\omega)\dot{Y}^{(i+1)}(\omega,t)\mathrm{d}\omega \\
&\quad + \cos\left(\frac{\alpha_i\pi}{2}\right) r^{\alpha_i}q^{(i)}(t) - r^2\int_0^\infty \mathrm{K}(\alpha_i,\omega)Y^{(i)}(\omega,t)\mathrm{d}\omega
\end{aligned} \qquad (4.8)
$$

for $i = 0,\ldots,n-1$ together with

$$
\dot{Y}^{(i)}(\eta,t) = q^{(i)}(t) - \eta Y^{(i)}(\eta,t), \quad Y^{(i)}(\eta,0) = \int_{t_0}^0 \mathrm{e}^{\eta\tau}q^{(i)}(\tau)\mathrm{d}\tau, \qquad (4.9)
$$

$i = 0,\ldots,n$, which is related to (2.9) and (4.1).

For a fixed value of α, the function $\mathrm{K}(\alpha,\cdot)$ has a maximum at

$$
\eta_{\max} = \sqrt{\frac{\alpha}{2-\alpha}}r. \qquad (4.10)
$$

Hence, the position of $\eta_{\max}$ may be adjusted by the magnitude of r. The graphs of $\mathrm{K}(\alpha,\eta)$ for different values of $\alpha \in (0,1)$ and $\eta_{\max} = 1$ (i.e.

$r^2 = \frac{2-\alpha}{\alpha}$) are displayed in Fig. 1. In the examples of Sect. 5, we consider geometrically distributed arguments $\eta_1, \dots, \eta_K$ centered at $10^0 = 1$ for the function $\mathrm{K}(\alpha, \cdot)$. Therefore, we choose $r^2 = \frac{2-\alpha}{\alpha}$ in Sect. 5, such that $\mathrm{K}(\alpha, \cdot)$ has its maximum at the central argument.

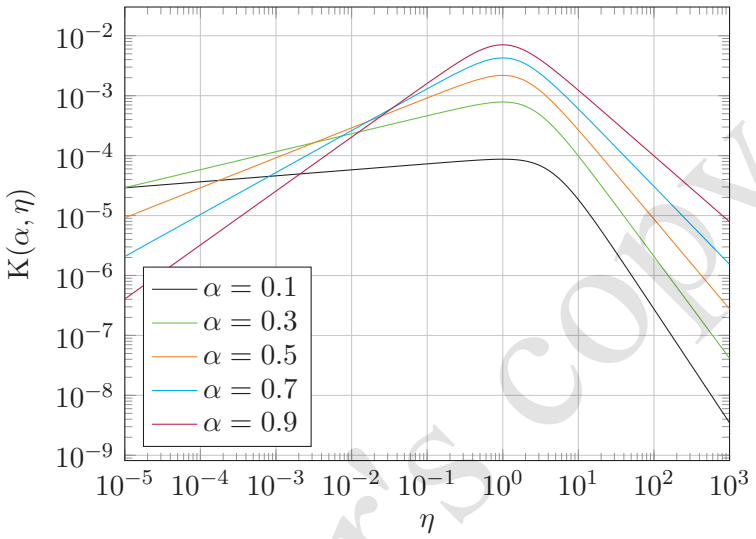

FIGURE 1. $\mathrm{K}(\alpha, \eta)$ for different values of $\alpha \in (0, 1)$.

4.2. **Derivation of the numerical scheme.** The key idea of our scheme is to approximate the integrals of the infinite states $Y^{(i)}$ and their derivatives in Eq. (4.8) by sums of a finite number of states $Y^{(i)}_{k,j}$, $k = 0, \dots, K-1$, $j = 1, \dots, J$ performing a composite Gaussian quadrature. The discretization of the infinite states creates two sources of error: the error in consequence of neglecting a part of the integration interval and the approximation error of the quadrature itself. In particular, we obtain an approximation

$$\begin{aligned} \int_0^\infty \mathrm{K}(\alpha_i, \omega) Y^{(i)}(\omega, t) \mathrm{d}\omega = &\sum_{k=0}^{K-1} \sum_{j=1}^{J} \mathrm{K}(\alpha_i, \eta_{k,j}) Y^{(i)}_{k,j}(t) w_{k,j} \\ &+ \mathrm{E}_1\left(Y^{(i)}(\cdot, t)\right) + \mathrm{E}_2\left(Y^{(i)}(\cdot, t)\right) \end{aligned} \tag{4.11}$$

for the integral of infinite states as may be found in (4.8) with errors

$$\mathrm{E}_1\left(Y^{(i)}(\cdot,t)\right) = \int_{\eta_K}^{\infty} \mathrm{K}(\alpha_i,\omega)Y^{(i)}(\omega,t)\mathrm{d}\omega, \tag{4.12}$$

$$\mathrm{E}_2\left(Y^{(i)}(\cdot,t)\right) = \int_{0}^{\eta_K} \mathrm{K}(\alpha_i,\omega)Y^{(i)}(\omega,t)\mathrm{d}\omega - \sum_{k=0}^{K-1}\sum_{j=1}^{J} \mathrm{K}(\alpha_i,\eta_{k,j})Y_{k,j}^{(i)}(t)w_{k,j}. \tag{4.13}$$

Thereby, similar as in Sect. 3.2 we choose $\eta_0 = 0, \eta_1, \ldots, \eta_K$ in $(0,\infty)$ and perform a Gaussian quadrature in each interval $(\eta_0,\eta_1),\ldots,(\eta_{K-1},\eta_K)$ with shifted Gauss-Legendre nodes

$$\eta_{k,j} = \frac{\eta_{k+1}-\eta_k}{2}s_j^{(0,0)} + \frac{\eta_k+\eta_{k+1}}{2} \in (\eta_k,\eta_{k+1}), \tag{4.14}$$

$j = 1,\ldots,J$, $k = 0,\ldots,K-1$ and weights

$$w_{k,j} = \frac{\eta_{k+1}-\eta_k}{2}w_j^{(0,0)},\ j = 1,\ldots,J,\ k = 0,\ldots,K-1 \tag{4.15}$$

related to the standard Gauss-Legendre nodes $s_j^{(0,0)}$ and weights $w_j^{(0,0)}$, $j = 1,\ldots,J$. To abbreviate, we denote $Y_{k,j}^{(i)}(t) := Y^{(i)}(\eta_{k,j},t)$, $j = 1,\ldots,J$, $k = 0,\ldots,K-1$. Accordingly, in an arbitrary FODE we can approximate a fractional derivative ${}^{C}D_{t_0+}^{\alpha_i}q^{(i)}(t)$ with (4.8) and (4.11) as

$$\begin{aligned}\widetilde{{}^{C}D_{t_0+}^{\alpha_i}q^{(i)}}(t) = \sin\left(\frac{\alpha_i\pi}{2}\right)r^{\alpha_i-1}q^{(i+1)}(t) - \sum_{k=0}^{K-1}\sum_{j=1}^{J}\mathrm{K}(\alpha_i,\eta_{k,j})\dot{Y}_{k,j}^{(i+1)}(t)w_{k,j}\\ + \cos\left(\frac{\alpha_i\pi}{2}\right)r^{\alpha_i}q^{(i)}(t) - r^2\sum_{k=0}^{K-1}\sum_{j=1}^{J}\mathrm{K}(\alpha_i,\eta_{k,j})Y_{k,j}^{(i)}(t)w_{k,j}.\end{aligned} \tag{4.16}$$

Hence, we approximate (2.5) by a system

$$\begin{aligned}&\left(A + B\sin\left(\frac{\alpha_{n-1}\pi}{2}\right)r^{\alpha_{n-1}-1}\right)q^{(n)}(t) - B\sum_{k=0}^{K-1}\sum_{j=1}^{J}\mathrm{K}(\alpha_{n-1},\eta_{k,j})\dot{Y}_{k,j}^{(n)}(t)w_{k,j}\\ &= \tilde{F}\left(t,q(t),\dot{q}(t),\ldots,q^{(n-1)}(t),\left(Y_{k,j}^{(0)}\right)_{k,j},\ldots,\left(Y_{k,j}^{(n)}\right)_{k,j}\right)\\ &\quad - B\cos\left(\frac{\alpha_{n-1}\pi}{2}\right)r^{\alpha_{n-1}}q^{(n-1)} + Br^2\sum_{k=0}^{K-1}\sum_{j=1}^{J}\mathrm{K}(\alpha_{n-1},\eta_{k,j})Y_{k,j}^{(n-1)}(t)w_{k,j}\end{aligned} \tag{4.17}$$

together with

$$\dot{Y}_{k,j}^{(i)}(t) = q^{(i)}(t) - \eta_{k,j} Y_{k,j}^{(i)}(t), \tag{4.18}$$

$i = 0, \dots, n,\ j = 1, \dots, J,\ k = 0, \dots, K-1$, related to (4.9). The system (4.17) may be transformed into a first-order ODE which together with (4.18) can be solved by a standard ODE-solver. Correspondingly, the initial function $q_0(t),\ t \in (t_0, 0)$ of the original FODE (2.5) has to be translated to initial values $Y_{k,j}^{(i)}(0)$ for the approximating ODE through

$$Y_{k,j}^{(i)}(0) = \int_{t_0}^{0} \mathrm{e}^{\eta_{k,j}\tau} q_0^{(i)}(\tau) \mathrm{d}\tau, \tag{4.19}$$

$i = 0, \dots, n,\ j = 1, \dots, J,\ k = 0, \dots, K-1$. In Sect. 5 we refer to the method proposed here as reformulated infinite state scheme (RISS).

Remark 4.2. The kernel $\mathrm{K}(\alpha, \eta)$ decays algebraically of order α to zero for $\eta \to 0$ such that the integrand is not differentiable at zero and the Gauss-Legendre approximation is of low order. However, the error may be controlled by choosing a small value for η_1 which we show in the next section. The advantage of a Gauss-Legendre quadrature in all subintervals (instead of a Gauss-Jacobi quadrature in $(0, \eta_1)$) is that only one set of weights and nodes can be used to discretize the infinite states $Y^{(i)}$, $i = 0, \dots, n$. Therefore, the number of states in (4.17) does not depend on the number of fractional derivatives in (2.5). Furthermore, an explicit FODE (2.5) leads to an explicit ODE (4.17) as approximation.

4.3. **Error analysis.** We restrict our analysis to the estimation of the error resulting from the discretization of the infinite states, i.e. (4.12), (4.13). For the truncation error E_1 we estimate the infinite states $Y^{(i)}$ using the solution of (4.9) in $[\eta_K, \infty)$ as

$$\begin{aligned} \left| Y^{(i)}(\eta, t) \right| &= \left| Y^{(i)}(\eta, 0)\mathrm{e}^{-\eta t} + \int_0^t \mathrm{e}^{-\eta(t-\tau)} q^{(i)}(\tau) \mathrm{d}\tau \right| \\ &\le C\mathrm{e}^{-\eta_K t} + \left\| q^{(i)} \right\|_\infty \int_0^t \mathrm{e}^{-\eta_K (t-\tau)} \mathrm{d}\tau \\ &\le C\mathrm{e}^{-\eta_K t} + \frac{\left\| q^{(i)} \right\|_\infty}{\eta_K} \end{aligned} \tag{4.20}$$

for some constant $C > 0$ and the uniform norm $\| \cdot \|_\infty$ in $[0, t]$. Using (4.20), for fixed $t \ge 0$ we obtain the estimation

$$\begin{aligned}\left|\mathrm{E}_1\left(Y^{(i)}(\cdot,t)\right)\right| &\le \left(C\mathrm{e}^{-\eta_K t}+\frac{\left\|q^{(i)}\right\|_\infty}{\eta_K}\right)\int_{\eta_K}^{\infty}\mathrm{K}(\alpha_i,\omega)\mathrm{d}\omega\\ &\le \left(C\mathrm{e}^{-\eta_K t}+\frac{\left\|q^{(i)}\right\|_\infty}{\eta_K}\right)\frac{\sin(\alpha_i\pi)}{\pi}\int_{\eta_K}^{\infty}\omega^{\alpha_i-2}\mathrm{d}\omega\\ &\le \left(C\mathrm{e}^{-\eta_K t}+\frac{\left\|q^{(i)}\right\|_\infty}{\eta_K}\right)\frac{\sin(\alpha_i\pi)}{\pi}\frac{\eta_K^{\alpha_i-1}}{1-\alpha_i}=\mathcal{O}\left(\eta_K^{\alpha_i-2}\right),\end{aligned} \tag{4.21}$$

which shows an algebraic decay of the truncation error for growing η_K. Furthermore, because of the exponential term in (4.21), we expect larger contributions of this term to the total error for time instants $t \ll \frac{1}{\eta_K}$.

To estimate the quadrature error, we decompose

$$\mathrm{E}_2\left(Y^{(i)}(\cdot,t)\right)=\sum_{k=0}^{K-1}\mathrm{E}_{2,k}\left(Y^{(i)}(\cdot,t)\right) \tag{4.22}$$

with

$$\begin{aligned}\mathrm{E}_{2,k}\left(Y^{(i)}(\cdot,t)\right) &= \int_{\eta_k}^{\eta_k+1}\mathrm{K}(\alpha_i,\omega)Y^{(i)}(\omega,t)\mathrm{d}\omega-\sum_{j=1}^{J}\mathrm{K}(\alpha_i,\eta_{k,j})Y_{k,j}^{(i)}(t)w_{k,j},\\ & k=0,\dots K-1,\end{aligned} \tag{4.23}$$

and introduce another estimation for $Y^{(i)}$ of the form

$$\begin{aligned}\left|Y^{(i)}(\eta,t)\right| &= \left|Y^{(i)}(\eta,0)\mathrm{e}^{-\eta t}+\int_0^t \mathrm{e}^{-\eta(t-\tau)}q^{(i)}(\tau)\mathrm{d}\tau\right|\\ &\le C+\left\|q^{(i)}\right\|_\infty\int_0^t \mathrm{d}\tau = C+\left\|q^{(i)}\right\|_\infty t,\end{aligned} \tag{4.24}$$

for some constant $C>0$ and the uniform norm $\|\cdot\|_\infty$ in $[0,t]$. For the first interval, as the integrand is not differentiable at zero, we use (4.24) to estimate for fixed $t \ge 0$

$$\begin{aligned}\left|\mathrm{E}_{2,0}\left(Y^{(i)}(\cdot,t)\right)\right| \le{}& \frac{\sin(\alpha_i\pi)}{\pi}\left(C+\left\|q^{(i)}\right\|_\infty t\right)\\ &\times\left(\int_0^{\eta_1}\frac{\omega^{\alpha_i}}{\omega^2+r^2}\mathrm{d}\omega+\sum_{j=1}^{J}\frac{\eta_{0,j}^{\alpha_i}}{\eta_{0,j}^2+r^2}w_{0,j}\right)\end{aligned}$$

$$\begin{aligned} &\leq \frac{\sin(\alpha_i\pi)}{\pi}\left(C+\left\|q^{(i)}\right\|_\infty t\right)\frac{\eta_1^{\alpha_i}}{r^2}\left(\int_0^{\eta_1}\mathrm{d}\omega+\sum_{j=1}^{J}w_{0,j}\right) \\ &= 2\frac{\sin(\alpha_i\pi)}{\pi}\left(C+\left\|q^{(i)}\right\|_\infty t\right)\frac{\eta_1^{1+\alpha_i}}{r^2}=\mathcal{O}(\eta_1^{1+\alpha_i}), \end{aligned} \tag{4.25}$$

where the next-to-last equality holds as the quadrature is exact for constant functions. The estimation (4.25) shows an algebraic decay of $|\mathrm{E}_{2,0}|$ for decreasing η_1 and the time-linear term in (4.25) leads to a larger contribution of this term to the total error for time instants $t \gg \frac{1}{\eta_1}$.

As the integrand is smooth in the other intervals, we can use an approximation theorem due to Jackson from [5, Chap. 4.8] similar as in [7, Thm. 9]. As stated in [5], an l-times continuously differentiable function $f \in C^l[a,b]$ may be approximated by a polynomial p_J of degree $\leq J$ as

$$|f(x)-p_J(x)| \leq C(l)\left(\frac{b-a}{J}\right)^l\left\|f^{(l)}(x)\right\|_\infty \tag{4.26}$$

for a constant $C(l)>0$ and the uniform norm $\|\cdot\|_\infty$ in $[a,b]$. As p_J can be integrated exactly using Gauss-Legendre quadrature, we obtain

$$\begin{aligned} \left|\mathrm{E}_{2,k}\left(Y^{(i)}(\cdot,t)\right)\right| &\leq \int_{\eta_k}^{\eta_{k+1}}\left|\mathrm{K}(\alpha_i,\omega)Y^{(i)}(\omega,t)-p_J(\omega)\right|\mathrm{d}\omega \\ &\quad+\sum_{j=1}^{J}\left|\mathrm{K}(\alpha_i,\eta_{k,j})Y_{k,j}^{(i)}(t)-p_J(\eta_{k,j})\right|w_{k,j} \\ &\leq 2C(l)(\eta_{k+1}-\eta_k)^{l+1}\left\|\frac{\mathrm{d}^l}{\mathrm{d}(\cdot)^l}\left(\mathrm{K}(\alpha_i,\cdot)Y^{(i)}(\cdot,t)\right)\right\|_\infty J^{-l}. \end{aligned} \tag{4.27}$$

Thereby, the interval length

$$\eta_{k+1}-\eta_k=\left(\left(\frac{\eta_K}{\eta_1}\right)^{\frac{1}{K-1}}-1\right)\eta_k \tag{4.28}$$

can be adjusted by the parameter K. The estimation (4.27) shows a rapid decay of the error for growing J but fixed K,η_1,η_K. However, if the ratio $\frac{\eta_K}{\eta_1}$ is increased, the parameter K has to be chosen large enough to bound the interval lengths (4.28) for large values of k.

Remark 4.3. To obtain small errors in (4.25), (4.27), the infinite states $Y^{(i)}(\eta,t)$, $i=0,\ldots,n$ have to be sufficiently smooth with respect to the first argument for $\eta\in(0,\infty)$. This requirement restricts the set of admissible initial functions. For $t_0 > -\infty$ there is no limitation as $q_0^{(i)}$,

$i = 0, \dots, n$ are bounded on $[t_0, 0]$ and hence

$$|Y^{(i)}(\eta, 0)| \leq \sup_{t\in[t_0,0]} |q^{(i)}(t)| \int_{t_0}^{0} \mathrm{e}^{\eta\tau} \mathrm{d}\tau = \sup_{t\in[t_0,0]} |q^{(i)}(t)| \frac{1 - \mathrm{e}^{\eta t_0}}{\eta}, \qquad (4.29)$$

which is finite even for $\eta \to 0$. In the case $t_0 = -\infty$ not every conceivable initial function leads to continuous infinite states. One example is a constant past $q_0 \equiv C$, $q_0^{(i+1)} \equiv 0$, $i = 0, \dots, n-1$, which leads to $Y^{(0)}(\eta, 0) = \frac{C}{\eta}$, which has a strong singularity in $\eta = 0$ such that Gauss-Legendre quadrature of $\int_0^\infty \mathrm{K}(\alpha, \omega) Y^{(0)}(\omega, 0) \mathrm{d}\omega$ fails.

In summary, we obtain the total error resulting from the discretization of the infinite states by the estimations (4.21), (4.25) and (4.27) which can be controlled by the quadrature parameters η_K, η_1 and J, K, respectively. The total error of the reformulated infinite state scheme results from the combined error of the infinite state discretization and the time-stepping method. The latter depends on the ODE solver used, which can be chosen independently from the infinite state discretization. The combined error is not in the scope of this paper.

5. **Benchmark problems**

In this section, we consider a number of benchmark problems, mainly of the form (2.5) equipped with initial functions. Most of the problems are inspired by those from [37, 38] sometimes with adapted initial conditions as the original problems do not fit the initial function approach or the fact mentioned in Rem. 4.3 leads to modification of the problems. In all the numerical examples we apply the reformulation (4.16) and choose $K = 25$ and $J = 10$ as parameters of quadrature, where η_k, $k = 1, \dots, K$ are logarithmically spaced in $[10^{-5}, 10^5]$, i.e.

$$\eta_1 = 10^{-5},\ \eta_K = 10^5,\ \eta_k = \eta_1 \left(\frac{\eta_K}{\eta_1}\right)^{\frac{k-1}{K-1}},\ k = 2, \dots, K. \qquad (5.1)$$

We state the resulting ODE and solve it using MATLAB's solver `ode15s.m` (absolute and relative tolerance at 10^{-8}), which uses certain backward differentiation formulas [31]. We compare the results to those of other methods mentioned in Sect. 3.

Benchmark Problem 1. We consider the simple one-term fractional differential equation with zero initial function given by

$$\begin{cases} {}^{C}D^{\alpha}_{-\infty+} q(t) = 1 - q(t), \\ \qquad\qquad q(t) = 0, \quad t \leq 0 \end{cases} \qquad (5.2)$$

with the closed form solution $q(t) = 1 - E_\alpha(-t^\alpha)$ (Fig. 2), where E_α is the one-parameter Mittag-Leffler function.

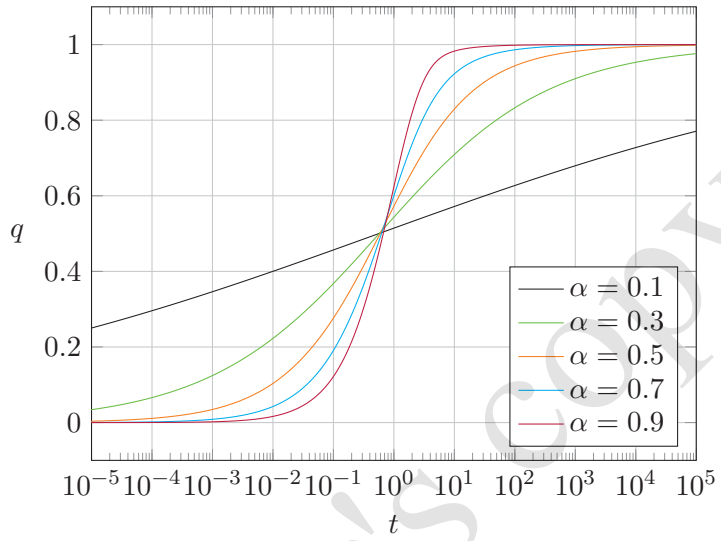

FIGURE 2. Benchm. 1: Analytical solution of (5.2) for various values of α.

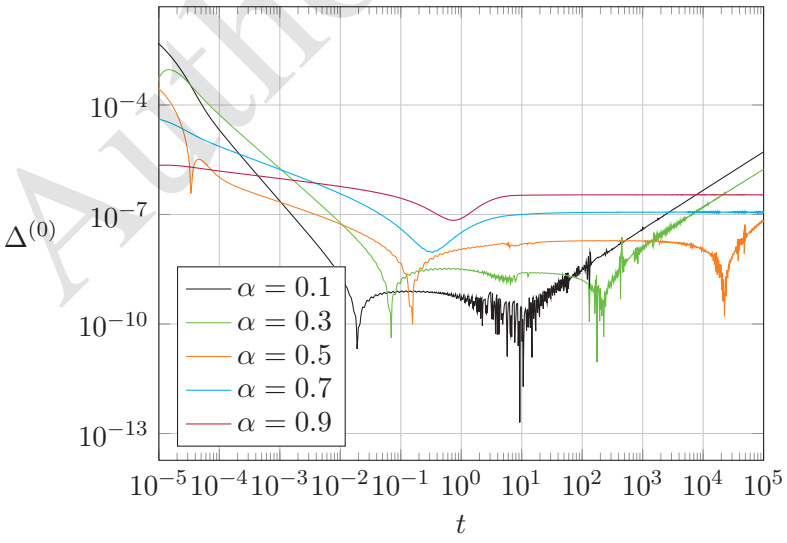

FIGURE 3. Benchm. 1: Absolute error of the numerical solution of (5.2) using RISS for various values of α.

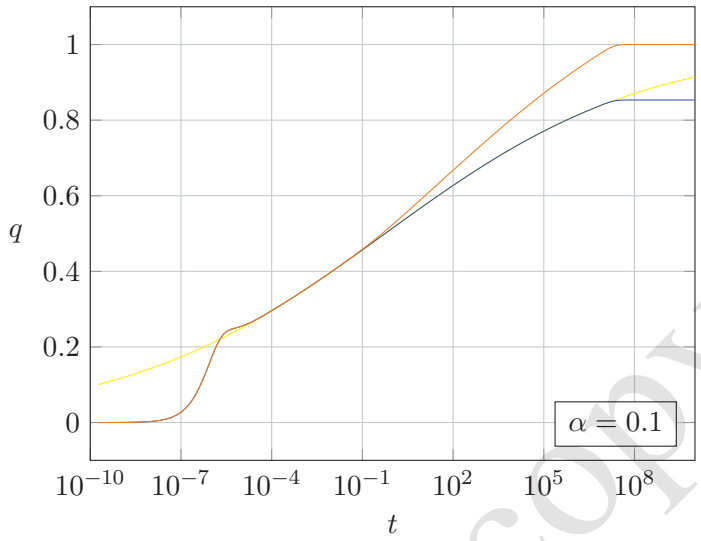

FIGURE 4. Benchm. 1: Analytical solution (yellow) and numerical solution using RISS (blue) and a scaled version of RISS (orange) with correct approximation of the asymptotic behavior of the solution for $\alpha = 0.1$.

Using (4.17), this problem may be approximated as

$$\begin{cases} \sin\left(\frac{\alpha\pi}{2}\right) r^{\alpha-1}\dot{q}(t) - \sum_{k=0}^{K-1}\sum_{j=1}^{J} \mathrm{K}(\alpha,\eta_{k,j})\dot{Y}_{k,j}^{(1)}(t)w_{k,j} \\ \quad = 1 - \left(1+\cos\left(\frac{\alpha\pi}{2}\right) r^{\alpha}\right) q(t) + r^2 \sum_{k=0}^{K-1}\sum_{j=1}^{J} \mathrm{K}(\alpha,\eta_{k,j}) Y_{k,j}^{(0)}(t) w_{k,j} \end{cases} \tag{5.3}$$

together with (4.18) and zero initial conditions in all states. The solution of (5.3) can be compared to the closed form solution of (5.2) for which the Mittag-Leffler function can be computed with the help of [13]. The absolute errors

$$\Delta^{(0)}(t) = |q(t) - \tilde{q}(t)| \tag{5.4}$$

between the exact solution $q(t)$ and its numerical approximation $\tilde{q}(t)$ are shown in Fig. 3 for many time scales. The results are generally good but show increasing static errors for small values of α for very small and very large time scales, i.e. the method leads to a wrong approximation of the asymptotic behavior of the solution. This phenomenon is in agreement with the estimations (4.21) and (4.25), which reveal increasing errors for small

and large t, respectively. In Fig. 4, we compare the solution of (5.3) for $\alpha = 0.1$ to a scaled version of it, where the last term in (5.3) is multiplied by a factor

$$\frac{\cos\left(\frac{\alpha\pi}{2}\right) r^{\alpha}}{r^2 \sum_{k=0}^{K-1} \sum_{j=1}^{J} \mathrm{K}(\alpha, \eta_{k,j}) \frac{1}{\eta_{k,j}} w_{k,j}},$$

such that the asymptotic behavior of the solution is correctly estimated. Unfortunately, the scaling leads to a larger error for smaller time scales and does not improve the approximation. We conclude, that RISS provides a good approximation of the solution of (5.2) only in a certain time interval. However, this interval can be extended by decreasing η_1 and increasing η_K together with an appropriate choice of J and K as explained in Sect. 4.3.

Furthermore, for $t \in (0, 100)$ we compare the results of RISS, ISS (applied to the fractional integral equation equivalent to (5.2)) and PC in Fig. 5. Thereby, we choose $J = 20$ for ISS such that the dimensions of the approximating ODEs in RISS and ISS are equal and we use a fixed step size $h = 5 \cdot 10^{-4}$ for PC as this choice leads to a similar computation time as for RISS with the parameters specified above. Fig. 5 shows a good performance of RISS for all chosen values of α while ISS works well only for large $\alpha \in (0, 1)$ and large time scales. The main reason for that seems to be the truncation error for ISS, which can be approximated similar as in (4.21), by

$$\begin{aligned} \left| \int_{\eta_K}^{\infty} \mu_\alpha(\omega) Z(\omega, t) \mathrm{d}\omega \right| & \\ \leq C \int_{\eta_K}^{\infty} \mu_\alpha(\omega) \mathrm{e}^{-\omega t} \mathrm{d}\omega + \|1 - q\|_\infty \int_{\eta_K}^{\infty} \frac{\mu_\alpha(\omega)}{\omega} \mathrm{d}\omega & \qquad (5.5) \\ \leq C \frac{t^{\alpha-1}}{\Gamma(\alpha)} + \|1 - q\|_\infty \frac{\sin(\alpha\pi)}{\alpha\pi} \eta_K^{-\alpha} & \end{aligned}$$

for some constant $C > 0$ and the uniform norm $\|\cdot\|_\infty$ in $[0, t]$ while the quadrature error for ISS can be estimated similar to (4.27). The error term in (5.5) has a large influence for small time scales, especially for $\alpha \to 0$ and is of lower order in η_K than the error in (4.21). In [1], such large errors can be avoided by splitting a local part of the fractional integral (2.3) before introducing the infinite state representation. The local part is then treated by an approximation method for Volterra integrals. For PC, we notice the improvement of the convergence behavior with increasing values of α corresponding to (3.7). Especially for large t, the absolute errors become smaller than for RISS. However, the computational costs for the used implementation of PC [12] behave like $\mathcal{O}\left(n \cdot \log(n)^2\right)$ with $n = \frac{T}{h}$

while RISS seems to work much more efficient. To see this, we present the relation between computation time and the mean absolute error $\bar{\Delta}^{(0)}$ for the three methods in Fig. 6. Therefore, we have increased the number J of quadrature nodes for fixed parameters $K = 25$, $\eta_1 = 10^{-5}$ and $\eta_K = 10^5$ for RISS ($J = 1, 2, 3, \ldots, 10$) and ISS ($\tilde{J} = 2J$) such that the dimensions of the resulting ODEs for RISS ($2KJ+1$) and ISS ($K\tilde{J}+1$) are equal and we have decreased the time step h for PC as $h = 10^{-\frac{J}{4}}$. For ISS, we obtain almost no reduction of the mean error for growing J. Apparently, the truncation error (5.5) is larger in magnitude than the quadrature error, which is reduced by increasing J. For RISS, we observe a steep decay of the mean error until $J = 7$. For larger values of J, the mean error remains almost the same as the error terms in (4.21) and (4.25) seem to predominate. For PC, we observe a slow decay of the error with increasing computation time such that RISS works more efficiently in the example given.

Remark 5.1. A slight change of (5.2) leads to an FODE with a non-zero constant initial function

$$\begin{cases} {}^{C}D^{\alpha}_{-\infty+} q(t) = -q(t), \\ \qquad\qquad q(t) = 1, \quad t \leq 0 \end{cases} \tag{5.6}$$

with the closed form solution $q(t) = E_\alpha(-t^\alpha)$. As $\dot{q}(t) = 0$ for $t < 0$, the fractional differential operator in (5.6) can as well be initialized at zero which leads to a classical non-zero initial condition $q(0) = 1$. As explained in Rem. 4.3, RISS is not suitable for such a problem, especially for $\alpha \to 0$ (Fig. 7). However, with the objective of modeling real systems, an infinite non-zero history seems inappropriate.

Benchmark Problem 2. Another one-term fractional differential equation with zero initial function adapted from [38] has the form

$$\begin{cases} {}^{C}D^{0.7}_{-\infty+} q(t) = f(t), \\ \qquad\qquad q(t) = 0, \quad t \leq 0 \end{cases} \tag{5.7}$$

with a piecewise defined right-hand side

$$f(t) = \begin{cases} \frac{1}{\Gamma(1.3)} t^{0.3}, & 0 \leq t \leq 1, \\ \frac{1}{\Gamma(1.3)} t^{0.3} - \frac{2}{\Gamma(2.3)} (t-1)^{1.3}, & t > 1. \end{cases} \tag{5.8}$$

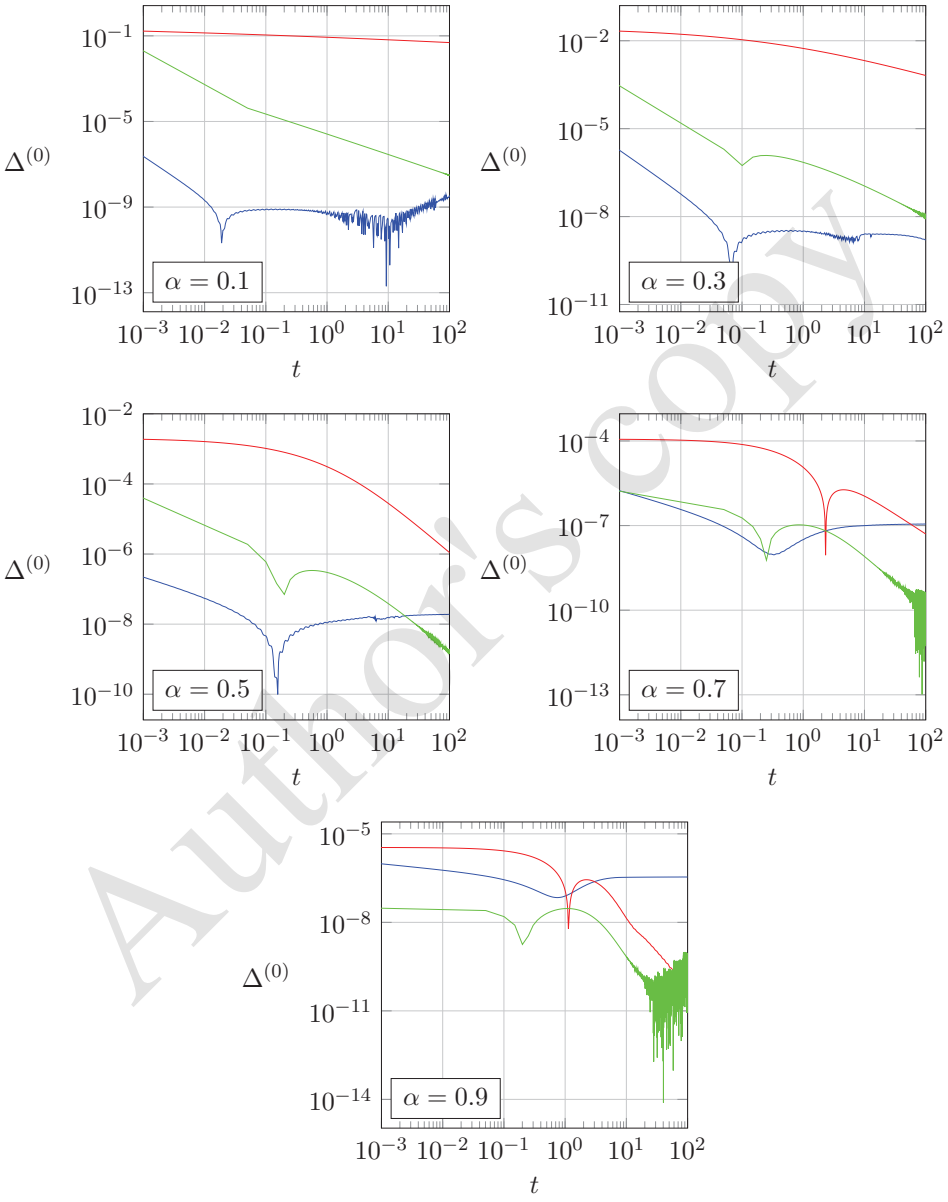

FIGURE 5. Benchm. 1: Absolute error of the numerical solution of (5.2) using RISS (blue), ISS (red) and PC (green) for various values of α.

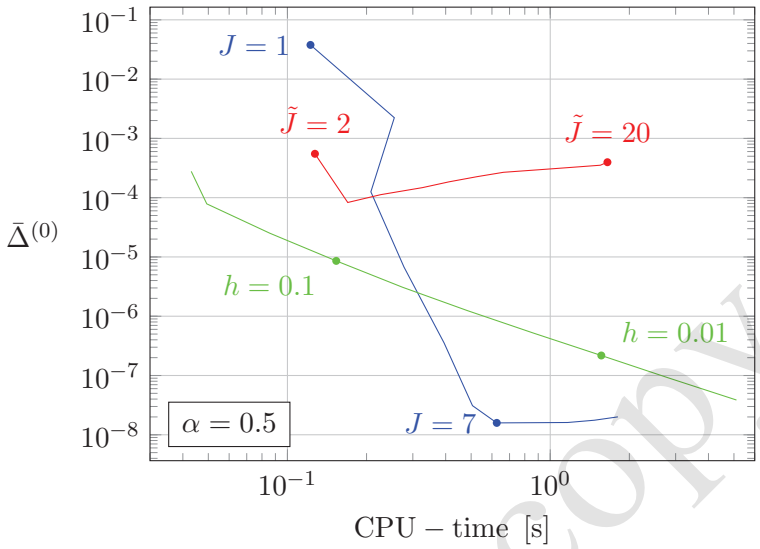

FIGURE 6. Benchm. 1: Work-precision diagram for RISS (blue), ISS (red) and PC (green) for $\alpha = 0.5$.

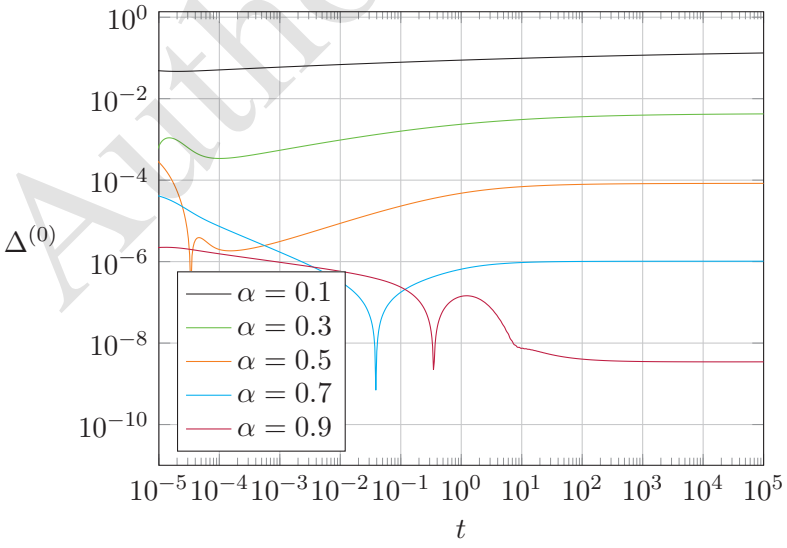

FIGURE 7. Benchm. 1: Absolute error of the numerical solution of (5.6) using RISS for various values of α.

The analytical solution of (5.7) is given by

$$q(t) = \begin{cases} t, & 0 \le t \le 1, \\ t - (t-1)^2, & t > 1 \end{cases} \tag{5.9}$$

in the interval $(0, 2)$. The approximation of (5.7) using (4.17) has the form

$$\begin{cases} \sin\left(\frac{7\pi}{20}\right) r^{-0.3} \dot{q}(t) - \sum_{k=0}^{K-1} \sum_{j=1}^{J} \mathrm{K}(0.7, \eta_{k,j}) \dot{Y}_{k,j}^{(1)}(t) w_{k,j} \\ \quad = f(t) - \cos\left(\frac{7\pi}{20}\right) r^{0.7} q(t) + r^2 \sum_{k=0}^{K-1} \sum_{j=1}^{J} \mathrm{K}(0.7, \eta_{k,j}) Y_{k,j}^{(0)}(t) w_{k,j}. \end{cases} \tag{5.10}$$

Again, the absolute errors using RISS, ISS and PC ($h = 5 \cdot 10^{-5}$) have been computed and the results may be found in Fig. 8. The step size for PC was again chosen such that the computation time of PC and RISS are similar. As in Benchm. 1, the best results can be obtained using RISS.

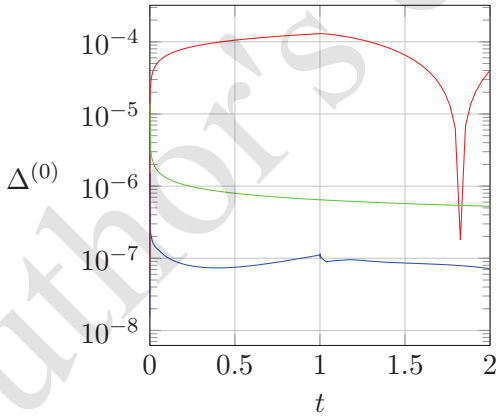

FIGURE 8. Benchm. 2: Absolute error of the numerical solution of (5.7) using RISS (blue), ISS (red) and PC (green).

BENCHMARK PROBLEM 3. We consider a third-order FODE adapted from the second problem in [38] of the form

$$\begin{cases} \dddot{q}(t) + {}^{C}D_{-\infty+}^{0.5} \ddot{q}(t) + \ddot{q}(t) + 4\dot{q}(t) + {}^{C}D_{-\infty+}^{0.5} q(t) + 4q(t) = 6\cos(t), \\ q(t) = \sqrt{2}\sin\left(t + \frac{\pi}{4}\right), \quad t \le 0, \end{cases} \tag{5.11}$$

which has the closed form solution $q(t) = \sqrt{2}\sin(t + \frac{\pi}{4})$ for $t > 0$. For the reformulation of (5.11) we have to introduce the infinite states $Y^{(i)}$,

$i = 0, \ldots, 3$ that fulfill (4.9). We apply (4.16) in (5.11) and obtain

$$\begin{cases} \left(1 + \dfrac{1}{\sqrt{2r}}\right) \dddot{q}(t) - \displaystyle\sum_{k=0}^{K-1} \sum_{j=1}^{J} \mathrm{K}(0.5, \eta_{k,j}) \dot{Y}_{k,j}^{(3)}(t) w_{k,j} \\ \quad + \left(1 + \dfrac{\sqrt{2r}}{2}\right) \ddot{q}(t) - r^2 \displaystyle\sum_{k=0}^{K-1} \sum_{j=1}^{J} \mathrm{K}(0.5, \eta_{k,j}) Y_{k,j}^{(2)}(t) w_{k,j} \\ \quad + \left(4 + \dfrac{1}{\sqrt{2r}}\right) \dot{q}(t) - \displaystyle\sum_{k=0}^{K-1} \sum_{j=1}^{J} \mathrm{K}(0.5, \eta_{k,j}) \dot{Y}_{k,j}^{(1)}(t) w_{k,j} \\ \quad + \left(4 + \dfrac{\sqrt{2r}}{2}\right) q(t) - r^2 \displaystyle\sum_{k=0}^{K-1} \sum_{j=1}^{J} \mathrm{K}(0.5, \eta_{k,j}) Y_{k,j}^{(0)}(t) w_{k,j} \\ = 6 \cos(t). \end{cases} \tag{5.12}$$

The initial function in (5.11) may be transferred to the initial values

$$Y^{(0)}(\eta, 0) = \int_{-\infty}^{0} e^{\eta\tau} q(\tau) \mathrm{d}\tau = \frac{\eta - 1}{1 + \eta^2}, \tag{5.13}$$

$$Y^{(1)}(\eta, 0) = \int_{-\infty}^{0} e^{\eta\tau} \dot{q}(\tau) \mathrm{d}\tau = \frac{\eta + 1}{1 + \eta^2}, \tag{5.14}$$

$$Y^{(2)}(\eta, 0) = \int_{-\infty}^{0} e^{\eta\tau} \ddot{q}(\tau) \mathrm{d}\tau = -\frac{\eta - 1}{1 + \eta^2}, \tag{5.15}$$

$$Y^{(3)}(\eta, 0) = \int_{-\infty}^{0} e^{\eta\tau} \dddot{q}(\tau) \mathrm{d}\tau = -\frac{\eta + 1}{1 + \eta^2} \tag{5.16}$$

of the infinite states. In Fig. 9 we show the absolute error

$$\Delta^{(2)}(t) = |q(t) - \tilde{q}(t)| + |\dot{q}(t) - \dot{\tilde{q}}(t)| + |\ddot{q}(t) - \ddot{\tilde{q}}(t)| \tag{5.17}$$

for $t \in (0, 1000)$ which has a maximal value $\Delta_{\max}^{(2)} \approx 10^{-6}$. Furthermore, we compare the results of RISS and PC ($h = 10^{-4}$) on the interval $t \in (0, 100)$. Apparently, RISS works slightly better than PC in this example while the computation time for PC is by a factor 3 higher than for RISS.

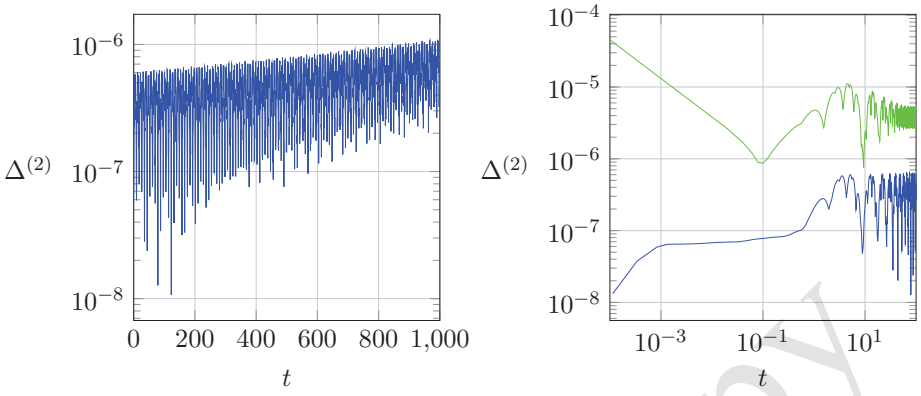

FIGURE 9. Benchm. 3: Absolute error of the numerical solution of (5.11) using RISS (blue) for $t \in (0, 1000)$ (left), $t \in (0, 100)$ (right) and PC for $t \in (0, 100)$ (green).

BENCHMARK PROBLEM 4. The nonlinear explicit FODE

$$\begin{cases} {}^{C}D^{\sqrt{2}-1}_{-\infty+}\dot{q}(t) = 2^{\sqrt{2}-0.5}\mathrm{e}^{-2t}q(t)\,{}^{C}D^{0.5}_{-\infty+}q(t) + 4\mathrm{e}^{4t} - \dot{q}^2(t) \\ q(t) = \mathrm{e}^{2t}, \quad t \leq 0 \end{cases} \tag{5.18}$$

with closed form solution $q(t) = \mathrm{e}^{2t}$ is adapted from the third problem in [38]. The associated ODE of the form (4.17) and the initial conditions of the infinite states can be derived as for the previous examples. For brevity, we only present the relative error

$$\Delta^{(1)}_{\mathrm{r}}(t) = \left|\frac{q(t) - \tilde{q}(t)}{q(t)}\right| + \left|\frac{\dot{q}(t) - \dot{\tilde{q}}(t)}{\dot{q}(t)}\right| \tag{5.19}$$

using RISS in Fig. 10 (left).

BENCHMARK PROBLEM 5. The nonlinear implicit FODE

$$\begin{cases} {}^{C}D^{0.2}_{-\infty+}q(t)\ {}^{C}D^{0.8}_{-\infty+}\dot{q}(t) + {}^{C}D^{0.3}_{-\infty+}q(t)\ {}^{C}D^{0.7}_{-\infty+}\dot{q}(t) = 8\mathrm{e}^{4t} \\ q(t) = \mathrm{e}^{2t}, \quad t \leq 0 \end{cases} \tag{5.20}$$

similar to the fourth problem in [38] with closed form solution $q(t) = \mathrm{e}^{2t}$ is not of the form (2.5). Nevertheless, we can introduce our reformulation (4.8), which leads to an implicit ODE that we can solve using MATLAB's `ode15i.m`. We present the relative error (5.19) in Fig. 10 (right).

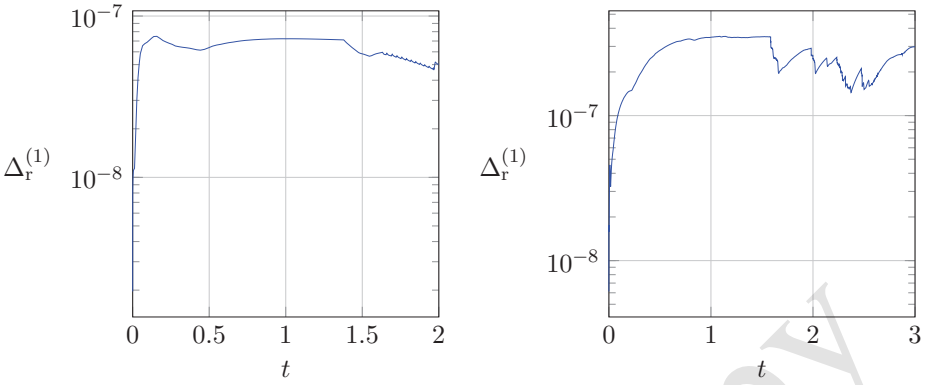

FIGURE 10. Benchm. 4 and 5: Relative error of the numerical solution of (5.18) (left) and (5.20) (right) using RISS.

6. **Conclusion**

The proposed numerical method for the simulation of fractional ordinary differential equations is based on the infinite state representation of fractional derivatives and uses a reformulation which leads to an integrable kernel $\mathrm{K}(\alpha, \eta)$, that is defined for $\alpha \in (0, 1)$ and $\eta \geq 0$ and does not have a weak singularity at $\eta = 0$. Therefore, we can approximate the occurring infinite state integrals all by the same quadrature of Gauss-Legendre type with reasonable errors that can be controlled by the quadrature parameters. This procedure transforms general FODEs to ODEs that can be solved by an ODE solver suitable for stiff ODEs. One advantage of the approach is the consideration of initial functions to correctly initialize fractional derivatives and its translation to initial values of the infinite states.

In comparison to a standard infinite state scheme (ISS, see Sect. 3.2) without reformulation, we obtain better results with our scheme for several benchmark problems, as the truncation error appears to decay much faster (compare (4.21) and (5.5)). The classical predictor-corrector scheme to solve fractional differential equations leads to similar results regarding the error as the reformulated infinite state scheme. However, especially for long-time simulation the computation time is much higher (see Fig. 6). Our method is applicable to a wide class of FODEs, i.e. even for nonlinear or fully implicit problems containing several fractional (even irrational-order) or integer-order operators. Moreover, the proposed scheme can be applied to problems containing variable-order fractional derivatives which leads to an explicitly time-dependent approximating ODE.

Acknowledgements

This work is supported by the Federal Ministry of Education and Research of Germany under Grant No. 01IS17096.

References

[1] D. Baffet, A Gauss-Jacobi kernel compression scheme for fractional differential equations. *J. of Scientific Computing* **79** (2019), 227–248.

[2] R. L. Bagley and P. J. Torvik, Fractional calculus in the transient analysis of viscoelastically damped structures. *AIAA Journal* **23** (1985), 918–925.

[3] T. A. Burton, *Stability and Periodic Solutions of Ordinary and Functional Differential Equations*. # 178, Academic Press (1985).

[4] A. Chatterjee, Statistical origins of fractional derivatives in viscoelasticity. *J. of Sound and Vibration* **284** (2005), 1239–1245.

[5] P. J. Davis and P. Rabinowitz, *Methods of Numerical Integration*, 2nd Ed. Ser. Computer Science and Applied Mathematics, Academic Press, New York (1984).

[6] K. Diethelm, *The Analysis of Fractional Differential Equations: An Application-Oriented Exposition Using Differential Operators of Caputo Type*. Ser. Lecture Notes in Mathematics, Springer, Berlin (2010).

[7] K. Diethelm, An investigation of some nonclassical methods for the numerical approximation of Caputo-type fractional derivatives. *Numerical Algorithms* **47** (2008), 361–390.

[8] K. Diethelm and N. J. Ford, Multi-order fractional differential equations and their numerical solution. *Applied Mathematics and Computation* **154** (2004), 621–640.

[9] K. Diethelm, N. J. Ford and A. D. Freed, A predictor-corrector approach for the numerical solution of fractional differential equations. *Nonlinear Dynamics* **29** (2002), 3–22.

[10] K. Diethelm, N. J. Ford and A. D. Freed, Detailed error analysis for a fractional Adams method. *Numerical Algorithms* **36** (2004), 31–52.

[11] D. Elliott, An asymptotic analysis of two algorithms for certain Hadamard finite-part integrals. *IMA J. of Numerical Analysis* **13** (1993), 445–462.

[12] R. Garrappa, Predictor-corrector PECE method for fractional differential equations. *MATLAB Central File Exchange* (2012), file ID: 32918.

[13] R. Garrappa, The Mittag-Leffler function. *MATLAB Central File Exchange* (2014), file ID: 48154.

[14] J. K. Hale, *Theory of Functional Differential Equations*, 2nd Ed. Ser. Appl. Math. Sci. # 3, Springer, N. York-Heidelberg-Berlin (1977).

[15] N. Heymans and J. C. Bauwens, Fractal rheological models and fractional differential equations for viscoelastic behavior. *Rheologica Acta* **33** (1994), 210–219.

[16] M. Hinze, A. Schmidt and R. I. Leine, Mechanical representation and stability of dynamical systems containing fractional springpot elements. *Proc. of the IDETC Quebec, Canada* (2018).

[17] M. Hinze, A. Schmidt and R. I. Leine, Lyapunov stability of a fractionally damped oscillator with linear (anti-)damping. *Internat. J. of Nonlinear Sci. and Numer. Simul.* (2019), Under review.

[18] S. Jiang, J. Zhang, Q. Zhang and Z. Zhang, Fast evaluation of the Caputo fractional derivative and its applications to fractional diffusion equations. *Commun. in Comput. Phys.* **21** (2017), 650–678.

[19] V. B. Kolmanovskii and V. R. Nosov, *Stability of Functional Differential Equations*. # 180, Elsevier (1986).

[20] J.-R. Li, A fast time stepping method for evaluating fractional integrals. *SIAM J. on Sci. Computing* **31** (2010), 4696–4714.

[21] C. F. Lorenzo and T. T. Hartley, Initialization of fractional-order operators and fractional differential equations. *J. of Comput. and Nonlinear Dynamics* **3** (2008), 021101–1–021101–9.

[22] C. Lubich, Discretized fractional calculus. *SIAM J. on Mathematical Analysis* **17** (1986), 704–719.

[23] D. Matignon, Stability properties for generalized fractional differential systems. *ESAIM: Proc.* **5** (1998), 145–158.

[24] G. Montseny, Diffusive representation of pseudo-differential time-operators. *ESAIM: Proc.* **5** (1998), 159–175.

[25] A. Oustaloup, *La Dérivation Non Entière: Théorie, Synthèse et Applications*. Hermès, Paris (1995).

[26] K. D. Papoulia, V. P. Panoskaltsis, N. V. Kurup and I. Korovajchuk, Rheological representation of fractional order viscoelastic material models. *Rheologica Acta* **49** (2010), 381–400.

[27] I. Podlubny, *Fractional Differential Equations*. Ser. Mathematics in Science and Engineering Vol. 198, Academic Press, San Diego (1999).

[28] H. Schiessel and A. Blumen, Hierarchical analogues to fractional relaxation equations. *J. of Phys. A: Mathematical and General* **26** (1993), 5057–5069.

[29] A. Schmidt and L. Gaul, On a critique of a numerical scheme for the calculation of fractionally damped dynamical systems. *Mechanics Research Commun.* **33** (2006), 99–107.

[30] A. Schmidt and L. Gaul, Finite element formulation of viscoelastic constitutive equations using fractional time derivatives. *Nonlinear Dynamics* **29** (2002), 37–55.

[31] L. Shampine and M. Reichelt, The MATLAB ODE Suite. *SIAM J. on Sci. Computing* **18** (1997), 1–22.

[32] S. J. Singh and A. Chatterjee, Galerkin projections and finite elements for fractional order derivatives. *Nonlinear Dynamics* **45** (2006), 183–206.

[33] J.-C. Trigeassou, N. Maamri, J. Sabatier and A. Oustaloup, State variables and transients of fractional order differential systems. *Computers and Math. with Appl.* **64** (2012), 3117–3140 (SI: Advances in FDE, III).

[34] J.-C. Trigeassou, N. Maamri, J. Sabatier and A. Oustaloup, A Lyapunov approach to the stability of fractional differential equations. *Signal Processing* **91** (2011), 437–445.

[35] J.-C. Trigeassou, N. Maamri, J. Sabatier and A. Oustaloup, Transients of fractional-order integrator and derivatives. *Signal, Image and Video Processing* **6** (2012), 359–372.

[36] Y. Wei, P. W. Tse, B. Du and Y. Wang, An innovative fixed-pole numerical approximation for fractional order systems. *ISA Trans.* **62** (2016), 94–102 (SI: Control of Renewable Energy Systems).

[37] D. Xue, *Fractional-order Control Systems - Fundamentals and Numerical Implementations*. Ser. Fractional Calculus in Applied Sciences and Engineering, De Gruyter, Berlin (2017).

[38] D. Xue and L. Bai, Benchmark problems for Caputo fractional-order ordinary differential equations. *Fract. Calc. Appl. Anal.* **20**, No 5 (2017), 1305–1312; DOI: 10.1515/fca-2017-0068; https://www.degruyter.com/view/j/fca.2017.20.issue-5/issue-files/fca.2017.20.issue-5.xml.

[39] L. Yuan and O. P. Agrawal, A numerical scheme for dynamic systems containing fractional derivatives. *J. of Vibration and Acoustics* **124** (2002), 321–324.

[1] *Institute for Nonlinear Mechanics*
University of Stuttgart
Pfaffenwaldring 9, 70569 Stuttgart, GERMANY

e-mail: hinze@inm.uni-stuttgart.de
schmidt@inm.uni-stuttgart.de
leine@inm.uni-stuttgart.de

Received: May 6, 2019

Please cite to this paper as published in:

Fract. Calc. Appl. Anal., Vol. **22**, No 5 (2019), pp. 1321–1350, DOI: 10.1515/fca-2019-0070; at https://www.degruyter.com/view/j/fca.